

## Quantum Lithography beyond the Diffraction Limit via Rabi Oscillations

Zeyang Liao,<sup>1</sup> M. Al-Amri,<sup>2</sup> and M. Suhail Zubairy<sup>1</sup>

<sup>1</sup>*Institute for Quantum Studies and Department of Physics and Astronomy, Texas A&M University, College Station, Texas 77843-4242, USA*

<sup>2</sup>*The National Center for Mathematics and Physics, KACST, P.O. Box 6086, Riyadh 11442, Saudi Arabia*  
(Received 3 May 2010; published 25 October 2010)

We propose a quantum optical method to do the subwavelength lithography. Our method is similar to the traditional lithography but adding a critical step before dissociating the chemical bound of the photoresist. The subwavelength pattern is achieved by inducing the multi-Rabi oscillation between the two atomic levels. The proposed method does not require multiphoton absorption and the entanglement of photons. It is expected to be realizable using current technology.

DOI: 10.1103/PhysRevLett.105.183601

PACS numbers: 42.50.St, 42.50.Ct, 42.50.Gy, 85.40.Hp

It is well known that the diffraction effects limit the feature size in optical lithography to half the wavelength of the light according to the Rayleigh criterion [1]. There is therefore interest in switching to a shorter wavelength to etch smaller patterns. However, when it comes to ultraviolet and x ray, the air and the traditional mirror begin to absorb light significantly [2]. Because of these and other problems, there is great interest in devising optical lithography schemes that can overcome the Rayleigh criterion.

Recently, several schemes [3–9] have been proposed to improve the spatial resolution of interferometric lithography beyond the diffraction limit. The approach based on quantum entanglement [3] requires entangled photon number states that are experimentally difficult to generate and sustain. In order to overcome this difficulty, several approaches have been developed to achieve the same level of resolution that are based on using classical light pulses [5,6]. These approaches, however, suffer from reduced visibility of generated structures. In an improved implementation of quantum lithography with classical light [8,9], subwavelength resolution was accomplished by correlating wave vector and frequency in a narrow band multiphoton detection process. These schemes are based on an  $N$ -photon absorption process and achieve a spatial resolution of  $\lambda/(2N)$ , where  $\lambda$  is the wavelength of the light. The indispensable requirement of a multiphoton transition, however, is accompanied by the need for high light field intensities, which makes an experimental realization of these schemes impractical. In [10], a novel method based on dark state physics was proposed to achieve the same spatial resolution  $\lambda/(2N)$  as previous schemes, but without requiring an  $N$ -photon absorption process. This scheme relies on the preparation of the system in a position dependent trapping state via phase shifted standing wave patterns and employs resonant atom-field interactions only. This method, however, requires multibeams and multilambda systems.

In this Letter, we propose a simple method to do subwavelength lithography which involves essentially two

atomic levels and does not require multiphoton absorption and/or the entanglement of the photons.

First, we briefly illustrate our method. We simplify the molecule as a three-level system (Fig. 1). Initially the molecules are in the ground state  $|b\rangle$ . Then we sequentially turn on two laser pulses with different frequencies. The first laser pulse, whose frequency is resonant with the energy difference between states  $|b\rangle$  and  $|a\rangle$ , will induce Rabi oscillations between these two states. After that we turn on the second laser pulse, and it will only dissociate the molecules that are in the excited states but not those in the ground states. The molecules that are dissociated will change their chemical properties, especially the solubility. The resulting patterns of the photoresist will thus depend on the spatial distribution of the excited state induced by the first laser pulse.

To achieve the subwavelength pattern, the first step is critical. Here we show how to prepare the molecules in a subwavelength position dependent state via coherent Rabi oscillations. Two beams of Gaussian pulses with the same frequency  $\nu_1$ , same maximal amplitude  $E_0$ , and same full width at half maximum of the intensity  $t_{\text{FWHM}} = 2\sqrt{\ln 2}\sigma$  are incident on the photoresist from opposite directions making an angle  $\theta$  with the horizontal. They then form a standing electric field described by

$$E(x, t) = 2E_0 \exp\left(-\frac{t^2}{2\sigma^2}\right) \cos(kx \cos\theta + \phi) \cos(\nu_1 t), \quad (1)$$

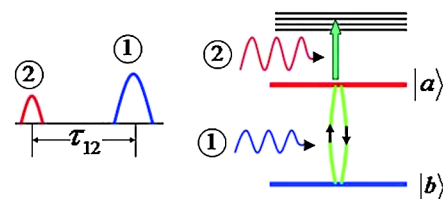


FIG. 1 (color online). Schematics for the proposed lithographic scheme.

where  $\phi$  is the phase difference between these two pulses and  $\nu_1$  is resonant with the  $|a\rangle \rightleftharpoons |b\rangle$  transition. The associated Rabi frequency is  $\Omega_R(x, t) = 2|\phi_{ba}|E_0 \exp(-\frac{t^2}{2\sigma^2}) \times \cos(kx \cos\theta + \phi)/\hbar$ , where  $\phi_{ba}$  is the electric dipole moment between levels  $|a\rangle$  and  $|b\rangle$  [11]. According to the area theorem, the upper-level probability after the pulse is

$$P_a(x) \simeq \frac{1 - \cos[\int_{-\infty}^{\infty} \Omega_R(x, t) dt]}{2} = \frac{1 - \cos[\Omega_0 t_0 \cos(kx \cos\theta + \phi)]}{2}, \quad (2)$$

where  $\Omega_0 = 2|\phi_{ba}|E_0/\hbar$  is the maximal Rabi frequency and  $t_0 = \sqrt{\pi/2 \ln 2} t_{\text{FWHM}}$ . From the equation, we see that the pattern is a double cosine function which depends on the pulse strength and pulse time.

We now look at the spatial pattern in more detail. For simplicity, we choose  $\theta = 0$  and  $\phi = 0$ . Then we have  $P_a(x) = (1 - \cos[\Omega_0 t_0 \cos(kx)]) / 2$ , from which we can calculate the positions of the valleys and the peaks. First, we note that the usual Rayleigh limit is obtained in the linear approximation corresponding to  $\Omega_0 t_0 \ll 1$ . In this case  $P_a(x) \approx \alpha [1 + \cos(2kx)]$  with  $\alpha = \Omega_0^2 t_0^2 / 8$  leading to a resolution of  $\lambda/2$ . Next we look at the situation where we are not restricted by the linear approximation and a number of Rabi oscillations during the pulse duration are allowed. When  $\Omega_0 t_0 = 4\pi$ , we have two Rabi cycles leading to a subwavelength pattern with a resolution of about  $\lambda/8$  [Fig. 2(b)]. Therefore it is, in principle, possible to achieve arbitrarily smaller subwavelength patterns using stronger field or increasing the pulse duration.

In a real system, decoherence time is an important factor. In Fig. 2, we numerically simulate the case when  $t_0 = \tau/2$ , where  $\tau$  is the decoherence time. We can see that while the visibility is reduced to about 85%, the resolution does not change. If the decoherence time decreases, we need to use shorter pulse and larger laser power to achieve the same resolution and the same visibility. However, in a practical situation, there is a limitation on the pulse duration and the pulse power. The contrast would be usually less than 100%.

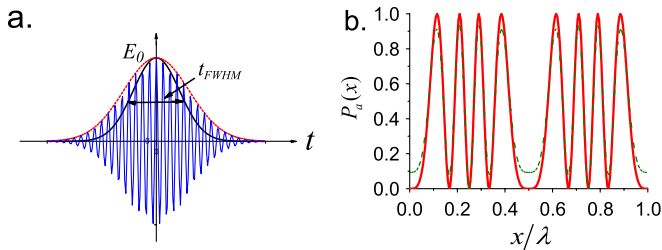


FIG. 2 (color online). (a) The Gaussian pulse. The red dashed line is the amplitude profile and the thick dark line is the intensity profile. (b) The pattern produced by the Gaussian pulse when  $\Omega_0 t_0 = 4\pi$ . The solid line is the result without the decoherence while the green dashed line shows the results with  $t_0 = \tau/2$ .

In general the patterns are nonperiodic [9,12,13]. We next discuss how the periodic patterns with a controllable harmonicity can be obtained. For the one-dimensional case, any functions in the range  $L$  can be expanded as a Fourier series:

$$f(x) = \frac{a_0}{2} + \sum_{n=1}^{\infty} \left[ a_n \cos\left(\frac{2n\pi x}{L}\right) + b_n \sin\left(\frac{2n\pi x}{L}\right) \right]. \quad (3)$$

For the components with periods  $L/n$  larger than optical wavelength  $\lambda$ , we just use the traditional techniques. For the components with  $L/n < \lambda$ , we apply our subwavelength scheme. We shine two phase locked pulses with amplitude  $E_0$  from angle  $\theta$  to form a standing wave and the third one with amplitude  $E_1$  from the right angle to form a constant background. The resulting electric field is  $E(x, t) = [2E_0 \cos(kx \cos\theta + \phi) + E_1] \exp(-\frac{t^2}{2\sigma^2}) \cos(\nu_1 t)$ . When  $\phi = \pi/2$  and  $n\pi - \epsilon \leq kx \cos\theta \leq n\pi + \epsilon$  ( $n$  is an integer and  $\epsilon$  is a small number),

$$E(x, t) \simeq [2E_0 kx \cos\theta + E_1] \exp\left(-\frac{t^2}{2\sigma^2}\right) \cos(\nu_1 t). \quad (4)$$

The gradient of intensity is approximately a constant in the regions  $(n\pi - \epsilon)/k \cos\theta \leq x \leq (n\pi + \epsilon)/k \cos\theta$ . This condition places restrictions on the choice of  $\theta$ . For example, to generate a sine pattern in a region  $10\lambda$ , with  $n = 0$  and  $\epsilon = \pi/4$ , we have  $\cos\theta = 1/40$ . The pattern produced in the linear region is

$$P_a(x) \simeq \frac{1 - \cos(Ax + B)}{2}, \quad (5)$$

where  $A = \Omega_0 t_0 k \cos\theta$  and  $B = \Omega_1 t_0$  with  $\Omega_1 = |\phi_{ab} E_1 / \hbar|$ . The coefficients  $A$  and  $B$  can be controlled by the field strengths and the pulse time. The effective wavelength  $\lambda_{\text{eff}} = \lambda / (\Omega_0 t_0 \cos\theta)$  can be made arbitrarily small by using stronger field or longer pulse duration. For  $\cos\theta = 1/40$ ,  $\lambda_{\text{eff}} = 40\lambda / \Omega_0 t_0$ . To reach a resolution of  $\lambda/10$ ,  $\Omega_0 t_0 = 400$ . If we ignore the constant background  $1/2$ , when  $B = 0$ , the pattern is a cosine function; when  $B = \pi/2$ , the pattern is a sine function.

We now discuss a possible system to implement our scheme. In the organic molecular photochemistry, the typical state energy diagram for the chemical bound is shown in Fig. 3 [14]. Here  $S_0$  and  $S_1$  are the ground singlet state and the first excited singlet state, respectively, and  $T_1$  is the first excited triplet state. As the transition between singlet state and the triplet state is dipole forbidden, the system is equivalent to a two-level system discussed above. In the figure,  $K_F$  is the fluorescence decay rate from  $S_1$  to  $S_0$ ,  $K_P$  is the phosphorescence decay rate from  $T_1$  to  $S_0$ , while  $K_{ST}$  is the intersystem crossing rate from  $S_1$  to  $T_1$ . To induce Rabi oscillations, the system should stay coherent. The typical decoherence time  $\tau$  is about 1–5 ps at room temperature due to the interactions between neighboring

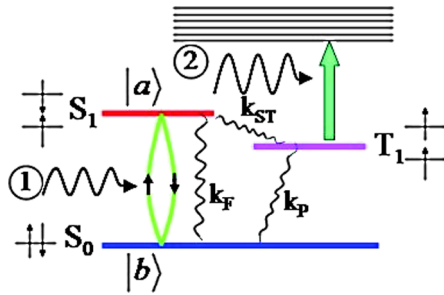


FIG. 3 (color online). The schematics for the state energy diagram for molecular organic photochemistry.

molecules [15]. To realize our subwavelength scheme, the requirements for these parameters are  $t_0 \sim \tau$  and  $K_{ST} \gg K_F \gg K_P$ . For  $K_{ST} \gg K_F$ , intersystem crossing from  $S_1$  to  $T_1$  dominates, which means that most of the molecules at  $S_1$  transfer to  $T_1$  instead of decaying to  $S_0$ . As the transition from  $T_1$  to  $S_0$  is spin forbidden, the lifetime (or phosphorescence time) of  $T_1$  is long. Within the phosphorescence time, we shine the second pulse to dissociate the molecules in state  $T_1$ . These requirements can be satisfied in some real systems. Usually, the time scale for  $K_F$  is  $10^5$ – $10^9$  Hz, for  $K_{ST}$  is  $10^5$ – $10^{11}$  Hz, and for  $K_P$  is  $10^{-2}$ – $10^3$  Hz. The Rabi frequency can be chosen as  $10^{12}$ – $10^{14}$  Hz. One example is 1-bromonaphthalene [14] for which  $K_F \sim 10^6$  Hz,  $K_{ST} \sim 10^9$  Hz,  $K_P \sim 30$  Hz. To generate a pattern with  $\lambda/10$  within the  $10\lambda$  region, we can choose  $t_0 = 5$  ps and  $\Omega_0 = 8 \times 10^{13}$  Hz. The corresponding peak power for the field  $E_0$  is  $2.17$  GW/cm<sup>2</sup> (with  $|\varphi_{ab}| = 10$  D [16]), which is smaller than  $4.7$  GW/cm<sup>2</sup> used in [17] and 3 orders of magnitude less than that used for two-photon fluorescence microscopy [18]. The lifetime of the intermediate state  $T_1$  is about 30 ms, which is long enough for us to shine the dissociation pulse. If the decoherence time of the system is 5 ps, the visibility is about 73%.

It is worthwhile to mention that dipole-dipole interaction or exchange interaction may induce energy transfer between neighboring molecules, which will limit the resolution in our scheme [14]. However, these effects can be ignored for the following reasons. The dipole-dipole energy transfer rate is of the order of fluorescence rate when the distance between two molecules is in the range of 1–5 nm. However, as we require  $K_{ST}$  to be much larger than  $K_F$ , the intersystem crossing to  $T_1$  will occur in times shorter than that required for the dipole-dipole energy transfer to the neighboring molecules. Also, when the molecules are in the triplet state the dipole-dipole energy transfer between the two molecules is forbidden. Therefore the energy transfer due to the dipole-dipole interaction can be ignored in our scheme. While the triplet-triplet energy transfer is allowed by the electron exchange interaction, it can only happen at a distance within 1 nm, which is about the size of the molecules. Usually we cannot reach such small patterns in the photoresist lithography.

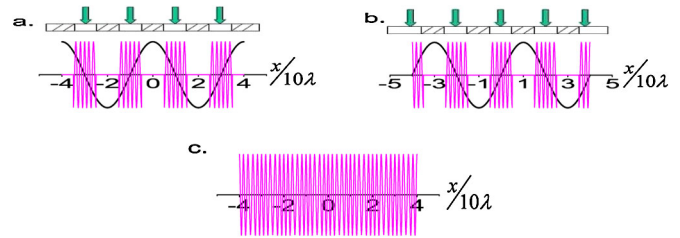


FIG. 4 (color online). A pictorial sketch for printing a sine pattern in an arbitrarily large region.

It is clear that a larger peak intensity would be required if the region over which the pattern is etched increases. For example, if we want to produce a sine pattern in the  $100\lambda$  region, the peak intensity requirement in the above example will be  $217$  GW/cm<sup>2</sup>, which may be very large and impractical. For large patterns (say, in the  $1000\lambda$  region), we propose a scheme as shown in Fig. 4. This scheme allows large patterns with the same peak intensity requirements as above. If we want to produce a sine pattern in a large region, we can do it in two steps. First, we shine the pulses from angle  $\theta$  and the period of the standing wave  $\lambda_{sw}$  is  $\lambda/\cos\theta$ . For example, if  $\cos\theta = 1/40$ , we have  $\lambda_{sw} = 40\lambda$ . The linear regions are distributed according to  $(20n - 5)\lambda \leq x \leq (20n + 5)\lambda$  (with  $\epsilon = \pi/4$ ) and the width of each linear region is  $10\lambda$ . We shine the second pulse through the mask with  $10\lambda$  holes to dissociate the molecules in these linear regions [Fig. 4(a)]. In the next step we shift the standing wave through a phase  $\pi/2$  such that the linear region also shifts a distance of  $10\lambda$ . This allows us to write the sine pattern in the remaining region [Fig. 4(b)]. After these two steps the resulting sine pattern can be formed [Fig. 4(c)]. The power requirement remains the same: to reach  $\lambda/10$  resolution, the peak power for the field  $E_0$  is about  $2.17$  GW/cm<sup>2</sup> (with  $|\varphi_{ab}| = 10$  D,  $t_0 = 5$  ps) and the peak power for the field  $E_1$  is about  $0.13$  MW/cm<sup>2</sup>.

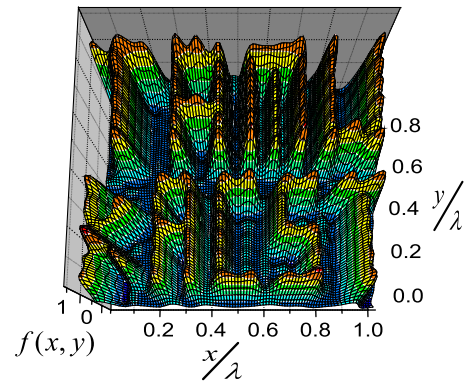


FIG. 5 (color online). A 2D pattern “TAMU-KACST” printed within one wavelength using the present method. Parameters are  $M = N = 15$ ,  $\theta = 80^\circ$ .

A novel feature of our scheme is that it may also be used to generate a nanopattern using a microwave field. For example, if two sublevels of a system have energy difference of about 3 GHz and the coherence time is of the order of 1 s, we can use a microwave pulse with wavelength 10 cm and pulse duration 0.1 s to induce the Rabi

oscillations between these two levels. If  $\Omega_R = 0.1$  GHz, the resolution could be of the order 10 nm.

We can also generalize our method to two-dimensional patterns. A function in the region  $\lambda \times \lambda$  can be simulated by the truncated Fourier series:

$$\begin{aligned}
 f(x, y) &= \sum_{m=0}^M \sum_{n=0}^N \left\{ a_{mn} \cos\left[\frac{2\pi(mx+ny)}{\lambda}\right] + b_{mn} \cos\left[\frac{2\pi(mx-ny)}{\lambda}\right] + c_{mn} \sin\left[\frac{2\pi(mx+ny)}{\lambda}\right] + d_{mn} \sin\left[\frac{2\pi(mx-ny)}{\lambda}\right] \right\} \\
 &\approx \sum_{m=0}^M \sum_{n=0}^N \left\{ a_{mn} \cos\left[\frac{\sqrt{m^2+n^2}}{\cos(\theta)} \cos\left[\frac{2\pi \cos(\theta)}{\lambda} \frac{(mx+ny)}{\sqrt{m^2+n^2}} + \frac{\pi}{2}\right]\right] + b_{mn} \cos\left[\frac{\sqrt{m^2+n^2}}{\cos(\theta)} \cos\left[\frac{2\pi \cos(\theta)}{\lambda} \frac{(mx-ny)}{\sqrt{m^2+n^2}} + \frac{\pi}{2}\right]\right] \right. \\
 &\quad \left. + c_{mn} \sin\left[\frac{\sqrt{m^2+n^2}}{\cos(\theta)} \cos\left[\frac{2\pi \cos(\theta)}{\lambda} \frac{(mx+ny)}{\sqrt{m^2+n^2}} + \frac{\pi}{2}\right]\right] + d_{mn} \sin\left[\frac{\sqrt{m^2+n^2}}{\cos(\theta)} \cos\left[\frac{2\pi \cos(\theta)}{\lambda} \frac{(mx-ny)}{\sqrt{m^2+n^2}} + \frac{\pi}{2}\right]\right] \right\}. \quad (6)
 \end{aligned}$$

From the first equation to the second, we have chosen  $\theta$  to be near  $90^\circ$ . Then  $\cos\left[\frac{2\pi \cos(\theta)}{\lambda} \frac{(mx+ny)}{\sqrt{m^2+n^2}} + \frac{\pi}{2}\right] \approx \frac{2\pi \cos(\theta)}{\lambda} \times \frac{(mx+ny)}{\sqrt{m^2+n^2}}$ . In a practical application, we should realize each Fourier component one by one. For the first and third components in Eq. (6) we shine the pulses from directions  $(m\hat{x} + n\hat{y})/\sqrt{m^2+n^2}$  while for the other two components we shine the pulses from directions  $(m\hat{x} - n\hat{y})/\sqrt{m^2+n^2}$  and  $\Omega_0 t_0 = \sqrt{m^2+n^2}/\cos(\theta)$ . In addition, due to the fact that the constant  $1/2$  appears in Eq. (3), there is an additional penalty deposition  $Q$  which depends on the Fourier coefficients. For example, applying the numerical simulation we print characters ‘‘TAMU-KACST’’ within one wavelength (Fig. 5). In the simulation, we take  $\theta = 80^\circ$  and  $M = N = 15$ .  $Q = 0.24h$ , where  $h$  is the height of the pattern. We have a total of  $15 \times 15 \times 4 = 900$  components, and each component needs four pulses (three for standing wave and one for dissociation). Therefore, we need 3600 pulses in total. Each component takes about 1 ms, and the whole process takes about 1 s. In our example, with the region  $\lambda \times \lambda$ , the required maximal power is about 200 MW/cm<sup>2</sup> for a pulse duration of  $t_0 = 5$  ps.

In conclusion, we have discussed a new quantum optical method to do subwavelength lithography which is realizable using current technology. This method makes use of Rabi oscillations between the two atomic levels. Our method relies on the nonlinearity of the atom-field interaction but does not require multiphoton absorption and/or photon entanglement.

This work is supported by grants from the King Abdulaziz City for Science and Technology (KACST) and from the Qatar National Research Fund (QNRF) under the NPRP project.

- [1] C. Mack, *Fundamental Optical Principles of Lithography: The Science of Microfabrication* (John Wiley & Sons Ltd., West Sussex, England, 2007).
- [2] C. Williams *et al.*, *Inf. Forsch. Ent.* **21**, 73 (2006).
- [3] A. Boto *et al.*, *Phys. Rev. Lett.* **85**, 2733 (2000).
- [4] M. D’Angelo, M. V. Chekhova, and Y. Shih, *Phys. Rev. Lett.* **87**, 013602 (2001).
- [5] G. S. Agarwal, R. W. Boyd, E. M. Nagasako, and S. J. Bentley, *Phys. Rev. Lett.* **86**, 1389 (2001).
- [6] A. Pe’er *et al.*, *Opt. Express* **12**, 6600 (2004).
- [7] S. J. Bentley and R. W. Boyd, *Opt. Express* **12**, 5735 (2004).
- [8] P. R. Hemmer, A. Muthukrishnan, M. O. Scully, and M. S. Zubairy, *Phys. Rev. Lett.* **96**, 163603 (2006).
- [9] Q. Sun, P. R. Hemmer, and M. S. Zubairy, *Phys. Rev. A* **75**, 065803 (2007).
- [10] M. Kiffner, J. Evers, and M. S. Zubairy, *Phys. Rev. Lett.* **100**, 073602 (2008).
- [11] M. O. Scully and M. S. Zubairy, *Quantum Optics* (Cambridge University Press, Cambridge, England, 1997).
- [12] S. Pau, G. P. Watson, and O. Nalamasu, *J. Mod. Opt.* **48**, 1211 (2001).
- [13] P. Kok *et al.*, *Phys. Rev. A* **63**, 063407 (2001).
- [14] N. J. Turro, V. Ramamurthy, and J. C. Scaiano, *Principles of Molecular Photochemistry: An Introduction* (University Science Books, Sausalito, CA, 2009).
- [15] S. F. Fischer and A. Laubereau, *Chem. Phys. Lett.* **35**, 6 (1975).
- [16] P. C. Becker *et al.*, *Phys. Rev. Lett.* **60**, 2462 (1988).
- [17] G. Donnert *et al.*, *Proc. Natl. Acad. Sci. U.S.A.* **103**, 11 440 (2006).
- [18] S. W. Hell and J. Wichmann, *Opt. Lett.* **19**, 780 (1994).